

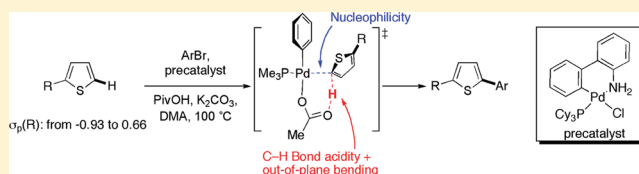
# Analysis of the Palladium-Catalyzed (Aromatic)C–H Bond Metalation–Deprotonation Mechanism Spanning the Entire Spectrum of Arenes

Serge I. Gorelsky,\* David Lapointe,\* and Keith Fagnou†

Department of Chemistry and Center for Catalysis Research and Innovation, University of Ottawa, 10 Marie Curie, Ottawa, ON, K1N 6N5 Canada

## Supporting Information

**ABSTRACT:** A comprehensive understanding of the C–H bond cleavage step by the concerted metalation–deprotonation (CMD) pathway is important in further development of cross-coupling reactions using different catalysts. Distortion–interaction analysis of the C–H bond cleavage over a wide range of (hetero)aromatics has been performed in an attempt to quantify the various contributions to the CMD transition state (TS). The (hetero)aromatics evaluated were divided in different categories to allow an easier understanding of their reactivity and to quantify activation characteristics of different arene substituents. The CMD pathway to the C–H bond cleavage for different classes of arenes is also presented, including the formation of pre-CMD intermediates and the analysis of bonding interactions in TS structures. The effects of remote C2 substituents on the reactivity of thiophenes were evaluated computationally and were corroborated experimentally with competition studies. We show that nucleophilicity of thiophenes, evaluated by Hammett  $\sigma_p$  parameters, correlates with each of the distortion–interaction parameters. In the final part of this manuscript, we set the initial equations that can assist in the development of predictive guidelines for the functionalization of C–H bonds catalyzed by transition metal catalysts.



## INTRODUCTION

Transition-metal-catalyzed functionalization of (hetero)arene C–H bonds has emerged over the past few years as a rapidly growing and increasingly reliable alternative to traditional cross-coupling reactions. The functionalization of a C–H bond generally depends on the growing array of compatible directing groups to access adjacent C–H bonds or relies on the intrinsic C–H bond reactivity toward catalysts.<sup>1</sup> In order to employ this transformation over a broad range of substrates and as part of increasingly more complex settings, it will require a more comprehensive understanding of the governing parameters influencing the reactivity and selectivity of the C–H bond cleavage step, especially for the approaches that do not use directing groups. In line with this objective, functionalities on aromatic rings such as fluorine,<sup>2,3</sup> chlorine,<sup>4</sup> trifluoromethyl, nitro,<sup>5,6</sup> nitrile,<sup>6</sup> and some ethers<sup>6,7</sup> were found over the years to impart an activating influence on C–H bonds toward functionalization reactions. Also, it was demonstrated that remote substituents at the C6 position of 1-methylindoles moderately affected the C2-arylation reactivity of the C–H bonds of these substrates.<sup>8</sup> Beyond searching for other activating groups, efforts aimed at better understanding of the reaction mechanism were made by categorizing the reactivity of arenes in terms of relative and absolute rates.<sup>9</sup>

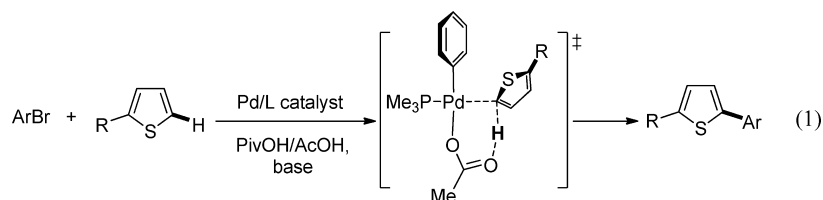
We are interested in developing reactivity guidelines in order to predict the regioselectivity of C–H bond functionalization with various arenes by extracting as much information as possible from previously investigated (hetero)aromatics.

Herein, we evaluate parameters that govern the activation barrier of the C–H bond cleavage *via* a concerted metalation–deprotonation (CMD) mechanism (eq 1) with palladium-carboxylate complexes for a diverse set of (hetero)arenes covering a wide spectrum of aromatic C–H coupling partners. We also identify and analyze various parameters that are common to all of the (hetero)arene C–H bond palladium-catalyzed reactions. We assess, both experimentally and computationally, the effect of substituents at a C2 position on the reactivity of C5–H bond of thiophenes. From this detailed analysis, we also set the basis of the guidelines that could eventually lead to a simple method that can be used to estimate the barriers of activation for a wide range of (hetero)arenes as well as to accurately predict the regioselectivity for all C–H functionalization reactions.

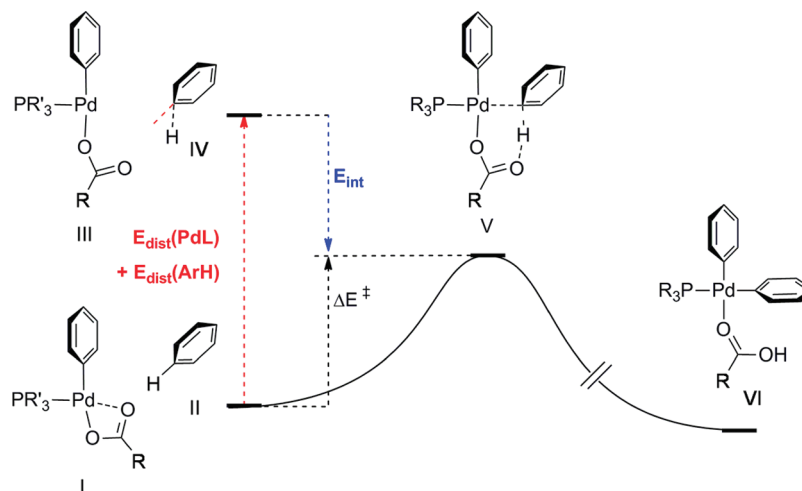
**Mechanistic Work Precedents.** Several previous investigations have focused on the understanding of the C–H bond cleavage mechanism on a wide range of systems, and from these studies, several different pathways have been proposed. The two mechanisms that have received the most attention are the electrophilic aromatic substitution ( $S_EAr$ ) and the CMD pathways.<sup>10,11</sup> Recently, Studer and Itami proposed a stepwise 1,2-migratory insertion mechanism to support the reversal in the regioselectivity caused by arylboronic acids in their report on the C4 arylation of thiophene and thiazole.<sup>12</sup> With respect

Received: November 16, 2011

Published: December 9, 2011



Scheme 1. Distortion–Interaction Analysis for the CMD Transition State; Benzene Is Shown as a Representative Substrate



to the CMD process, the earliest C–H bond cleavage mechanistic studies by metal-carboxylate complexes began in the 1980s,<sup>13</sup> and the first computational study with palladium was reported in 2000.<sup>14</sup> These studies however were limited to benzene metalation.

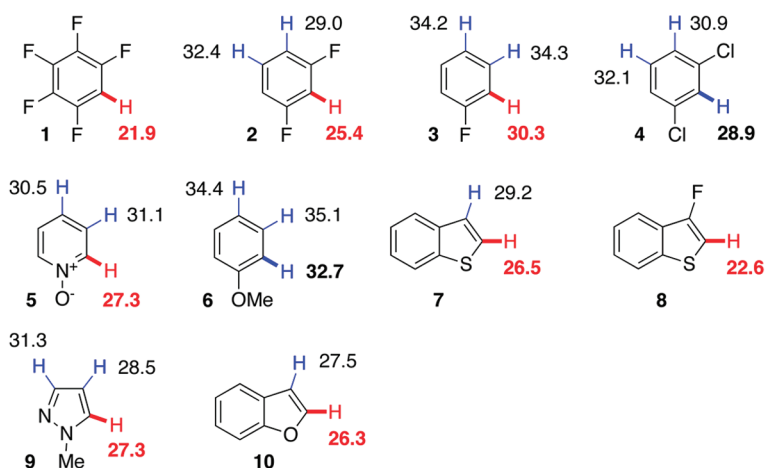
Recent mechanistic studies on the palladium-catalyzed direct arylation were conducted on various systems, including benzene,<sup>15,16</sup> tethered diarenes,<sup>2,7,17</sup> as well as electron-deficient arenes, such as fluorobenzenes<sup>3</sup> and azine-*N*-oxides.<sup>9</sup> The results of these studies supported the concerted metalation–deprotonation mechanism with the participation of an inner- or outer-sphere base.<sup>11</sup> However, until recently it was generally accepted that electron-rich heteroarenes reacted through a  $S_EAr$  mechanism due to their high nucleophilicity. In 2008, we demonstrated that the C–H bond cleavage for a wide range of (hetero)arenes, including electron-rich (hetero)arenes, by the Pd<sup>II</sup>-acetate complex proceed by the CMD pathway.<sup>18</sup> The calculated activation barriers predicted accurately the regioselectivity observed experimentally for the palladium-catalyzed direct arylation of each (hetero)arene evaluated. For the oxidative cross-coupling of indole with benzene,<sup>19</sup> both C–H bond cleavages were explained by the same mechanism.<sup>20</sup> Tan and Hartwig recently demonstrated that the C–H bond cleavage of benzene by the Pd<sup>II</sup> catalyst with a DMA ligand has a lower CMD activation barrier than the C–H bond cleavage with the phosphine analogue.<sup>16</sup> This finding points to future opportunities in the development of better Pd<sup>II</sup> catalysts for C–H bond functionalization. Nonetheless, the phosphine ligand is used in a majority of the direct coupling reactions reported in the literature. It was experimentally demonstrated that the calculated barriers of activation for the CMD mechanism are also in agreement with the relative reactivity of the various (hetero)arenes.<sup>21</sup> As a result, one can utilize the values of CMD activation barriers to determine the site-selectivity of direct coupling reactions where two or more heteroarenes are present within a single substrate.

## RESULTS AND DISCUSSION

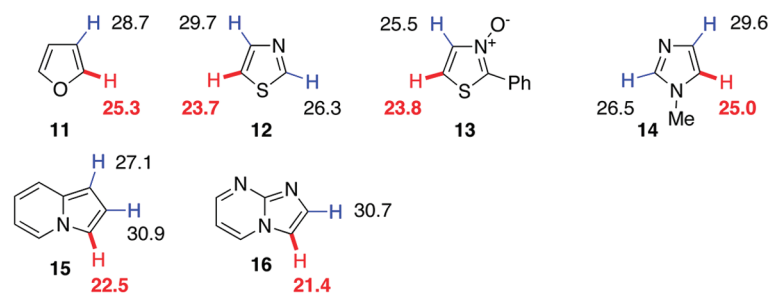
To gain a better understanding of how the CMD mechanism might be applicable to a disparate range of (hetero)arenes, a distortion–interaction analysis was performed for every C–H bond of selected aromatics.<sup>22</sup> This analysis quantifies different contributions to the CMD barrier V (Scheme 1). On one hand there is the energetic cost (distortion energy,  $\Delta E_{\text{dist}}$ ) associated with the distortion of the palladium complex and the arene from their ground state structures (I and II) to their geometries (III and IV) in the TS structure V. On the other hand, there is the energy gain (interaction energy,  $\Delta E_{\text{int}}$ ) resulting from the electronic interaction of fragments III and IV to form the TS structure V.

To evaluate the parameters governing the palladium-catalyzed C–H bond cleavage, (hetero)arenes 1–22h were selected to represent a range of (hetero)arenes spanning the entire spectrum of C–H coupling partners (Figure 1, Table S1 in Supporting Information). The mechanism of the C–H bond metalation by a palladium-acetate complex of each arene was evaluated by density functional theory (DFT) with the B3LYP<sup>23</sup> exchange-correlation functional. Even though some of the arenes chosen were part of our original computational study,<sup>18</sup> eight additional nonthiophene substrates (2, 3, 4, 6, 9, 10, 18, 19) and nine C2 substituted thiophenes (22a–j) were included in order to increase the scope of the study. For each substrate, a lowest-energy transition state corresponding to the CMD pathway was located. Pd<sup>II</sup>-catalyzed C–H bond functionalization of arene 4 is the only example on this list that has not been reported experimentally<sup>24</sup> and yet it has been demonstrated that a chlorine substituent has C–H bond activating properties similar to those of a fluorine substituent.<sup>4</sup> While solvent corrections were not employed, the relative barriers of activation on each of the (hetero)arenes employed (1–22h) matched the experimental regioselectivity for all cases except anisole (6).<sup>25</sup> The CMD activation barriers for C–H bond cleavage of anisole were found to be dependent on the

## Class I



## Class II



## Class III

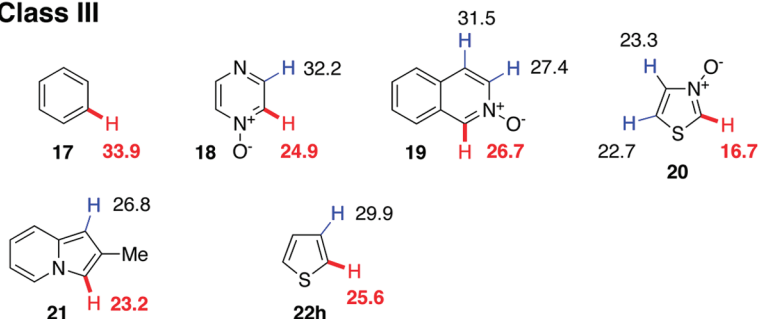


**Figure 1.** Free energy of activation ( $\Delta G_{298K}^\ddagger$ , kcal mol<sup>-1</sup>) for C–H bond functionalization *via* the CMD pathway with the [Pd(C<sub>6</sub>H<sub>5</sub>)(PMe<sub>3</sub>)(OAc)] catalyst. Red bonds correspond to the experimentally observed sites of arylation<sup>26</sup> except for arene 4.<sup>27</sup>

inclusion of solvent effects. For example, the CMD activation barriers for anisole in acetonitrile are 40.9:42.2:40.6 kcal mol<sup>-1</sup> for *o*:*m*:*p* C–H bonds, respectively, whereas the corresponding barriers in the gas phase are 32.7:35.1:34.4 kcal mol<sup>-1</sup>.

Values of Gibbs free energy barriers show good correlation with electronic energy barriers (Figure S1 in Supporting Information). The former are higher than the latter due to the entropic factor,  $T\Delta S$  (free substrate and catalyst form a transition state complex reducing the number of species by one).

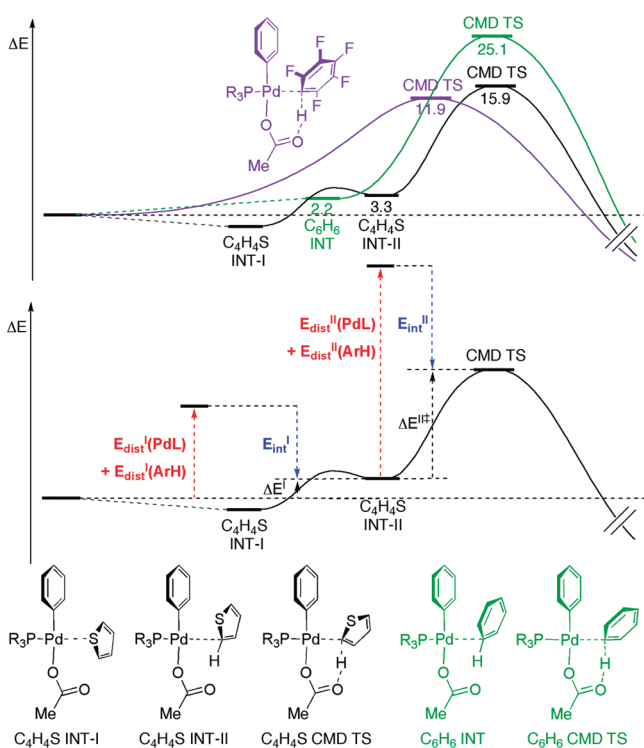
The distortion–interaction analysis for CMD TS structures for each C–H bonds of arenes **1**–**22h** revealed several factors that influence the regioselectivity of palladium-acetate catalyzed functionalization reactions. These factors allowed for the classification of the arenes into three categories (Scheme 1, Table S1). We have categorized to Class I arenes, for which the regioselectivity of C–H bond functionalization is controlled by

the difference in the (hetero)arene distortion energies,  $\Delta E_{\text{dist}}(\text{ArH})$ . An example of such an arene is benzothiophene (**7**) for which C<sub>α</sub>–H bonds are more reactive than C<sub>β</sub>–H bonds in the CMD process due to lower arene distortion energy at the C<sub>α</sub> site (37.5 kcal mol<sup>-1</sup> for C<sub>α</sub> arylation vs 39.8 kcal mol<sup>-1</sup> for C<sub>β</sub> arylation, Table S1). In Class II are included the (hetero)arenes for which interaction energies,  $\Delta E_{\text{int}}$  are the determining factor that define the most reactive C–H bond. An example of such an arene is furan (**11**) for which C<sub>α</sub>–H bonds are more reactive than C<sub>β</sub>–H bonds in the CMD process due to more negative interaction energy at the C<sub>α</sub> site (–44.8 kcal mol<sup>-1</sup> for C<sub>α</sub> arylation vs –40.0 kcal mol<sup>-1</sup> for C<sub>β</sub> arylation, Table S1). The (hetero)arenes in which both the distortion and interaction energies influence the choice of the C–H bond with the lowest barrier of activation are part of Class III compounds. An example of such arene is thiophene **22h** for which C<sub>α</sub>–H bonds are more reactive than C<sub>β</sub>–H bonds in the CMD process

due to lower arene distortion energy at the  $C_\alpha$  site (39.9 kcal mol<sup>-1</sup> for  $C_\alpha$  arylation vs 41.8 kcal mol<sup>-1</sup> for  $C_\beta$  arylation, Table S1) and more favorable interaction energy at the  $C_\alpha$  site (-41.4 kcal mol<sup>-1</sup> for  $C_\alpha$  arylation vs -37.8 kcal mol<sup>-1</sup> for  $C_\beta$  arylation, Table S1). This classification of the (hetero)arenes helps to better understand arylation regioselectivity for these substrates.

**Detailed DFT Analysis of the Process Leading to CMD ( $\pi$ -Complexes).** Previous mechanistic work on C-H bond functionalization of simple arenes demonstrated the formation of  $\kappa_1$ ,  $\eta_1$ , or  $\eta_2$   $\pi$ -complexes between the arene with the metal-carboxylate complex prior to the cleavage of the C-H bond.<sup>11,14,18,28</sup> Computationally such intermediates are typically obtained with electron-rich heteroarenes such as thiophene (Scheme 2, black pathway). Benzene has also previously been

**Scheme 2. CMD Pathways for C-H Bond Cleavage in Various Arenes<sup>a</sup>**



<sup>a</sup> $C_6F_5H$ , purple;  $C_6H_6$ , green;  $C_4H_4S$ , black.

shown to form a  $\pi$ -complex intermediate (Scheme 2, green pathway).<sup>14,28</sup> The distortion-interaction analysis for these  $\pi$ -complex intermediates (Table 1) reveals that the major energy cost for the formation of these structures comes from the distortion of the metal complex ( $\Delta E_{\text{dist}}^I(\text{PdL})$ ) as well as the

entropic loss. The geometries of arenes are not significantly perturbed in the structures of the  $\pi$ -complexes, as can be seen from very low values of the arene distortion energies ( $\Delta E_{\text{dist}}^I(\text{ArH}) \leq 1.4$  kcal mol<sup>-1</sup>). The only factor favoring the formation of these intermediates is the electronic interaction between the Pd<sup>II</sup> atom with an open coordination site and the  $\pi$ -electrons of the arenes. From the pre-CMD intermediate, the TS can easily be accessed with diminished energetic cost ( $\Delta E_{\text{dist}}^{II}(\text{PdL})$  and  $\Delta E_{\text{dist}}^{II}(\text{ArH})$  in Table 1).

However, not every arene can form a  $\pi$ -complex intermediate. When undergoing the Pd<sup>II</sup>-catalyzed C-H bond cleavage, pentafluorobenzene (1), an electron-deficient arene, does not go through the formation of the  $\pi$ -complex intermediate. The analysis of the reaction pathway reveals that, when this arene approaches the empty coordination site of the palladium central atom, an interaction with the carbon of the arene C-H bond and the interaction of the C-H bond proton with the base ligand lead into the CMD process (Scheme 2, purple pathway). For this substrate, no potential energy minimum corresponding to the  $\pi$ -complex intermediate was detected in the reaction pathway before the C-H bond cleavage transition state.

### Metalation-Deprotonation: Concerted or Not?

Throughout the mechanistic studies performed in regards to C-H bond cleavage of various (hetero)arenes by metal-carboxylate complexes, quite often these studies were proposing either the stepwise  $S_{\text{E}}\text{Ar}$  mechanism or a single-step concerted process. Sames and co-workers proposed an intermediary process for the C5 functionalization of *N*-SEM-imidazoles, the electrophilic metalation-deprotonation (EMD) mechanism.<sup>29</sup> This proposal goes along with the idea of a possible continuum for the mechanisms of the C-H bond cleavage by transition metal-carboxylate complexes. At one end of this continuum lies a "pure" stepwise  $S_{\text{E}}\text{Ar}$  pathway in which the metal-carbon bond is fully formed before the C-H bond cleavage occurs. On the other end would reside a fully concerted process in which the metal-carbon bond is formed at the same time as the C-H bond is cleaved. The mechanism of C-H bond functionalization of each (hetero)arene with different transition-metal catalysts can fall in between these two limiting scenarios. To verify this proposal, we have prepared a More O'Ferrall-Jencks diagram,<sup>30</sup> in which both the O-H and M-C bond formations and the C-H bond breaking at the CMD transition state for (hetero)arenes 1-22h (Figure 2 and Figure S2 in Supporting Information) are characterized by Mayer bond orders for the corresponding bonds.

At the transition state with the Pd<sup>II</sup>-acetate catalyst, the bond orders of the forming O-H bonds are narrowly situated in the 0.52-0.59 range. The Pd-C and C-H bond orders are more dependent on the nature of the arene; particularly the

**Table 1. Gibbs Free Energies and Electronic Energies of Pre-CMD Intermediates for the Lowest-Energy CMD Pathway with ArH Substrates and [Pd( $C_6H_5$ )(PMe<sub>3</sub>)(OAc)] Catalyst, Catalyst and Substrate Distortion Energies, Difference between Distortion Energies for CMD Transition States and Pre-CMD Intermediates, and Metal-Arene Interaction Energies (kcal mol<sup>-1</sup>)**

arene	$\Delta G_{298K}$	$\Delta E^I$	$E_{\text{dist}}^I(\text{PdL})$	$E_{\text{dist}}^I(\text{ArH})$	$E_{\text{int}}^I$	$E_{\text{dist}}^{II}(\text{PdL})^a$	$E_{\text{dist}}^{II}(\text{ArH})^a$	$E_{\text{int}}^{IIa}$
17	14.0	2.2	9.4	0.4	-7.6	7.0	44.2	-28.3
22h	14.8	3.3	12.9	1.0	-10.7	4.4	38.9	-30.7
22c <sup>b</sup>	14.1	2.3	13.4	1.4	-12.5	4.2	38.2	-30.9
11	11.7	-1.0	12.3	0.8	-14.2	5.5	41.7	-30.6

<sup>a</sup>See Scheme 2 for notations and Table S1 for  $E_{\text{dist}}$  values for CMD TS structures. <sup>b</sup>2-Fluorothiophene; see Figure 3.



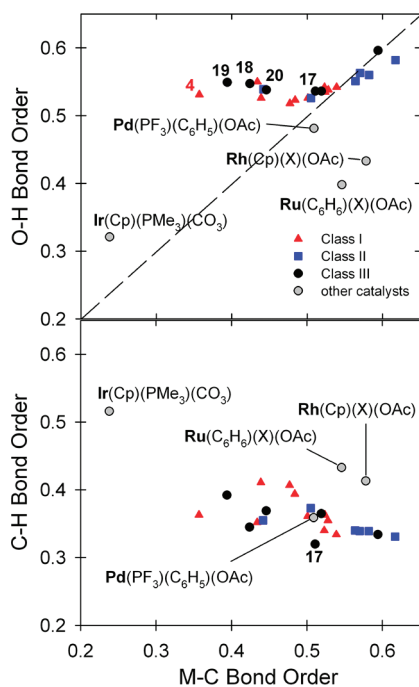


**Figure 2.** Metal–C(arene), (base ligand)O–H and C–H(arene) bond orders for the lowest-energy CMD TS structures for arenes 1–22h with the [Pd(C<sub>6</sub>H<sub>5</sub>)(PMe<sub>3</sub>)(OAc)] catalyst (red triangles for Class I arenes, blue squares for Class II arenes, and black circles for Class III arenes) and with the other catalysts (gray circles) [Pd(C<sub>6</sub>H<sub>5</sub>)(PF<sub>3</sub>)(OAc)] and [Ir(C<sub>3</sub>H<sub>5</sub>)(PMe<sub>3</sub>)(CO<sub>3</sub>)] (benzene is the substrate)<sup>31</sup> and the intramolecular CMD for the [Rh(C<sub>3</sub>H<sub>5</sub>)(X)(OAc)] and [Ru(C<sub>6</sub>H<sub>6</sub>)(X)(OAc)] complexes,<sup>32,35</sup> where X is the arene substrate (phenylpyridine for Ru and N-hydroxybenzamide for Rh) bound to the central metal through the N atom. The dashed line represents the expected trend for the perfectly concerted formation of M–C and O–H bonds.

Pd–C(arene) bond orders spread from 0.36 to 0.62, which is still fairly narrow. The distribution of the C–H bond orders in

the TS structures are also narrow (from 0.32 to 0.41), but taking into consideration the diversity of the nature of the C–H bonds and the important proximity to the Pd–C bond formation process, they all are similar TSs. In general, Class I arenes exhibited weaker Pd–C bonding interactions in the CMD TS structures of the (hetero)arenes investigated fit into a fairly narrow region in both 2-dimensional representations of the 3-dimensional More O’Ferrall–Jencks diagram. Thus, fairly small deviation of data points (O–H bond orders vs M–C bond orders) from the expected trend for the concerted formation of the M–C and O–H bonds (the dashed line in Figures 2 and S2) for different arenes do not provide support for the idea of significant continuum of mechanisms for the arene C–H bond cleavage using the Pd<sup>II</sup>-carboxylate catalysts.

To compare the dependence of the CMD process with respect to the nature of the metal catalyst, the transition states of arene C–H bond cleavage were calculated for iridium(III),<sup>31</sup> rhodium(III),<sup>32</sup> and ruthenium(II).<sup>33</sup> The CMD TS structure with the Ir<sup>III</sup>-carbonate catalyst has a high synchronicity for the formation of the O–H and Ir–C bonds, although the TS occurs very early in the progression of the metal–benzene interaction. Rhodium(III) and ruthenium(II) are known to be fairly electrophilic, and this is reflected by the increased metal–carbon bonding interaction over the O–H bond at the CMD TS structures with the Rh<sup>III</sup>- and Ru<sup>II</sup>-acetate catalysts. Overall, the metalation–deprotonation process presents a high level of synchronicity in the formation of the metal–carbon and O–H bonds (dashed line in Figure 2), which is in contrast to the formation of a  $\sigma$ -complex (Wheland intermediate) in a S<sub>E</sub>Ar process. The Wheland intermediate, a signature of a S<sub>E</sub>Ar process, would exhibit a fully formed M–C bond with the C–H bond left intact.

**Thiophenes.** Previous mechanistic work on the mechanism of direct arylation has highlighted the effect of a remote

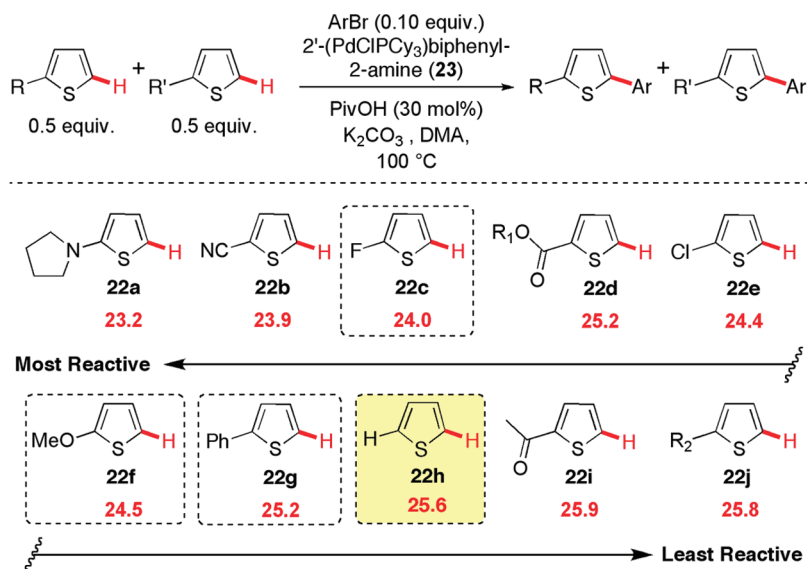


**Figure 3.** Experimentally observed relative reactivity of C2-substituted thiophenes (except for the substrates inside boxes (22c, 22f, 22g, 22h) for which competition experiments could not be carried, see main text for clarifications). Values in red correspond to the Gibbs free energy of activation ( $\Delta G_{298K}^\ddagger$ , kcal mol<sup>-1</sup>) for the CMD pathway with the [Pd(C<sub>6</sub>H<sub>5</sub>)(PMe<sub>3</sub>)(OAc)] catalyst. R<sub>1</sub> = *i*-Pr was modeled as Me. R<sub>2</sub> = *n*-Pr was modeled as Me.

substituent on the reactivity of C–H bonds.<sup>8</sup> The arylation of thiophenes under standard CMD reaction/catalyst conditions always results in functionalization of C<sub>α</sub>–H bonds (Figure 1). To gain a better understanding of the effect of substituents, we chose to focus our attention on the C5 functionalization of C2-substituted thiophenes. These thiophenes reacted in good yields under standard direct arylation reaction conditions without optimizations,<sup>26b</sup> although we employed a variation of a precatalyst [2'-Pd(PCy<sub>3</sub>)Cl-2-aminobiphenyl] (23), developed by Buchwald and co-workers.<sup>34</sup> Competition experiments (Figure S3 in Supporting Information) provided the data required for comparison of the experimental reactivity of these thiophenes with the calculated barriers of C–H bond cleavage at the C5 position (Figure 3). Considering the limitations of the DFT calculations and the inherent experimental variability of the competition reactions, the experimental and theoretical results are in good agreement. Unfortunately, not every thiophene in Figure 3 could be tested because of either reactivity or availability issues. For instance, the competition reactions with 2-methoxythiophene (22f) could not be taken into consideration in the reactivity chart, since 22f was incompatible with the reactions conditions when tested individually (less than 10% yield). The unsubstituted thiophene 22h could not be employed in the competition reactions because although it reacted very well under the standard conditions, the arylation product (22g) was significantly more reactive than the parent thiophene, and so a substantial quantity of double arylation product was formed.<sup>35</sup>

The observed reactivity of substituted thiophenes (Figure 3) is not in agreement with S<sub>E</sub>Ar reactivity. Thiophenes with electron-withdrawing groups at the C2 position such as nitrile (22b) and ester (22e) were found (experimentally and computationally) to be the most reactive substrates along with thiophene containing the strongly electron-donating *N*-pyrrolidine substituent (22a). Thiophene with a weak electron-donating group such as a propyl chain (22j) was found experimentally to be the least reactive substrate along with the thiophene possessing the acetyl substituent (22i).

The distortion–interaction analysis of the CMD TS structures for thiophenes casts light on the influence of the substituents on both the distortion energy of the arene and the arene–catalyst interaction energy (Table 2). Highly  $\pi$ -nucleophilic

**Table 2. Distortion–Interaction Analysis (kcal mol<sup>-1</sup>) for CMD TS Structures of C2-Substituted Thiophenes with the [Pd(C<sub>6</sub>H<sub>5</sub>)(PMe<sub>3</sub>)(OAc)] Catalyst**

Entry	Thiophene	C2 substituent	$\Delta G^\ddagger_{298K}$	$\Delta E^\ddagger$	$E_{\text{dist}}(\text{PdL})^a$	$E_{\text{dist}}(\text{ArH})$	$E_{\text{int}}$
1	22a	-NC <sub>4</sub> H <sub>8</sub>	23.2	12.3	20.0	47.6	-55.3
2	22b	-CN	23.9	14.1	16.4	34.8	-37.1
3	22c	-F	24.0	13.8	17.6	39.6	-43.4
4	22d	-Cl	24.4	14.3	17.4	37.9	-41.0
5	22f	-OMe	24.5	14.0	18.5	42.4	-46.9
6	22e	-CO <sub>2</sub> R <sub>1</sub> <sup>b</sup>	25.2	15.6	17.8	37.3	-39.5
7	22g	-Ph	25.2	15.3	17.4	39.3	-41.4
8	22h	-H	25.6	15.9	17.3	39.9	-41.4
9	22j	-R <sub>2</sub> <sup>c</sup>	25.8	15.6	17.8	40.7	-42.9
10	22i	-Ac	25.9	16.0	16.4	36.5	-37.0

<sup>a</sup>Distortion energy for the [Pd(C<sub>6</sub>H<sub>5</sub>)(PMe<sub>3</sub>)(OAc)] catalyst. <sup>b</sup>R<sub>1</sub> = *i*-Pr was modeled as Me. <sup>c</sup>R<sub>2</sub> = *n*-Pr was modeled as Me.

thiophenes, such as 22a and 22f, benefit from more negative  $E_{\text{int}}$ , although this effect is partially counterbalanced by an increase in the arene distortion energy,  $E_{\text{dist}}(\text{ArH})$ . Electron-withdrawing groups, such as acetyl (22i), ester (22e), fluorine

(22c), and nitrile (22b), reduce the energetic penalties for the arene distortions but also reduce the magnitude of the interaction energy between the substrate and the catalyst.

A closer examination of the distortion–interaction parameters revealed a correlation with the nature of the C2 substituent. Indeed, the expression of  $-E_{\text{int}}$  as a function of Hammett  $\sigma_p$  constants<sup>36</sup> for the substituent highlights the relationship between the  $\pi$ -nucleophilicity of the arenes and their interaction with the palladium–acetate catalyst (Figure 4, blue

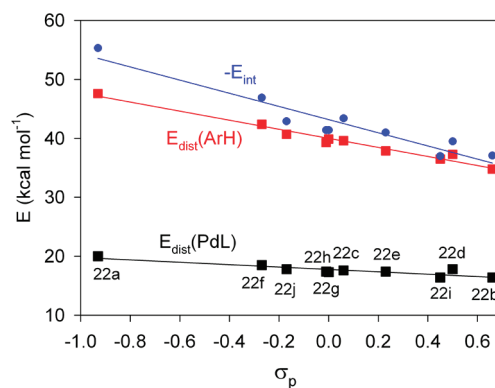


**Figure 4.** Distortion–interaction parameters (kcal mol<sup>-1</sup>) for the Pd<sup>II</sup>-catalyzed CMD transition states as a function of  $\sigma_p$  values for C2 substituted thiophenes. The solid lines show the linear correlations.

circles). As mentioned before, the beneficial effects of electron-donating groups on the  $E_{\text{int}}$  values are partially offset by the increased  $E_{\text{dist}}(\text{ArH})$  penalties (Figure 4, red squares). Figure 4 puts in contrast these two factors. The third factor is  $E_{\text{dist}}(\text{PdL})$  (Figure 4, black squares). The small dependence of  $E_{\text{dist}}(\text{PdL})$  on the arene nucleophilicity can be rationalized by the fact that arenes with high nucleophilicity and, thus, more negative  $E_{\text{int}}$  are expected to cause greater structural distortion of the metal–acetate catalyst to accommodate the incoming substrate.

Using the linear regression for the distortion–interaction parameters in Figure 4 we obtain:

$$E_{\text{dist}}(\text{ArH}) = 40.0(2) - 7.7(4)\sigma_p \quad (2)$$

$$E_{\text{dist}}(\text{PdL}) = 17.8(2) - 2.0(4)\sigma_p \quad (3)$$

$$E_{\text{int}} = -43.2(5) + 11(1)\sigma_p \quad (4)$$

Although correlations with Hammett parameters have previously been employed in the C–H bond cleavage mechanistic studies with various systems, including simple arenes,<sup>37</sup> indoles,<sup>8</sup> and pyridine-*N*-oxides,<sup>9</sup> to the best of our knowledge this is the first time that Hammett  $\sigma_p$  constants are shown to be linked to the  $E_{\text{dist}}(\text{ArH})$  and  $E_{\text{int}}$  factors. Unfortunately, the current  $\sigma_p$  model derived from eqs 2–4 for thiophenes 22a–j does not allow accurate evaluation of CMD activation barriers (Figure S4 in Supporting Information) due to accumulation of parameter errors.

**Efforts toward the Establishment of Predictable Arene C–H Bond Functionalization Guidelines.** As mentioned in the introduction, we are interested in deriving general trends from a wide array of (hetero)arenes with a final objective of developing reactivity guidelines for predicting the regioselectivity of C–H bond functionalization of various (hetero)arenes.

**Arene Distortion Energy.** The energy cost associated with the distortion of the arenes into their CMD transition state geometry can be separated into two components: (1) the C–H bond elongation and (2) the out-of-plane bending of the C–H bond of the arene. Evaluation of the C–H bond elongation and out-of-plane bending of the C–H bond as contributions to  $E_{\text{dist}}(\text{ArH})$  for each arene (Figure 5) demonstrated that the out-

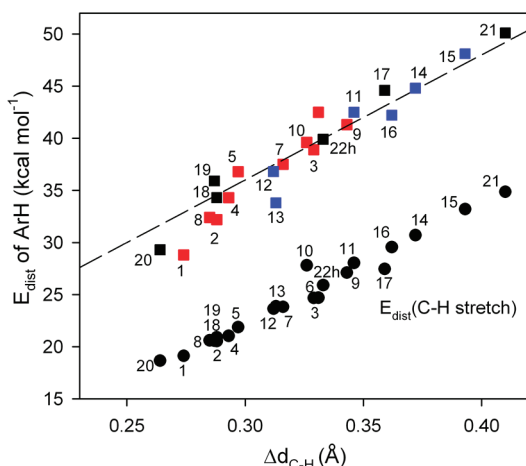


**Figure 5.** Arene distortion energies (squares; red for Class I arenes, blue for Class II arenes, and black for Class III arenes) and the C–H bond distortion energies (circles) for the lowest-energy CMD TS structures with the  $[\text{Pd}(\text{C}_6\text{H}_5)(\text{PMe}_3)(\text{OAc})]$  catalyst as a function of the C–H bond elongation for different arene substrates.

of-plane bending contribution to the arene distortion energy is, in fact, fairly constant (the average value  $13.2 \text{ kcal mol}^{-1}$  with a standard deviation of  $2.2 \text{ kcal mol}^{-1}$  derived from the distortion energy values for 22 arenes in Figure 5).

As shown in Figure 2, the C–H bond orders in the CMD TS structures with the  $\text{Pd}^{\text{II}}$  catalyst revealed that for all the arenes the C–H bond orders are in a narrow range (0.32–0.41, the mean value is 0.36). This information would simplify the evaluation of arene distortion energies, if one could take the energy cost to elongate a C–H bond to a distance that corresponds to the bond order of  $\sim 0.36$  in free arene and add this value to the out-of-plane bending “constant”,  $13.2 \text{ kcal mol}^{-1}$ . Unfortunately, this procedure cannot be applied because the hydrogen atom of the C–H bond in the TS structure also interacts with the base ligand (acetate). In the absence of the interaction with the base ligand, the C–H bond order would be considerably higher than  $\sim 0.36$  for the same bond elongation and would exhibit significant variation in bond orders (Table S3).

Nonetheless, the estimation of arene distortion energies can be made using the deprotonation energies of the C–H bonds of free arenes (Figure 6). The C–H bond deprotonation energy,  $E_{\text{deprotonation}}$ , could be easily calculated by removing the proton from the corresponding C–H bond of the arene and optimizing the structure of the resulting anion. For Class I substrates, the linear regression analysis of the correlation between  $E_{\text{dist}}(\text{ArH})$  and  $E_{\text{deprotonation}}$  leads to an approximate expression:

$$E_{\text{dist}}(\text{ArH}) = 0.37(5)E_{\text{deprotonation}} - 107(21) \quad (5)$$

Figure 6 also indicates that the correlation established for Class I arenes works fairly well for all Class III arenes except

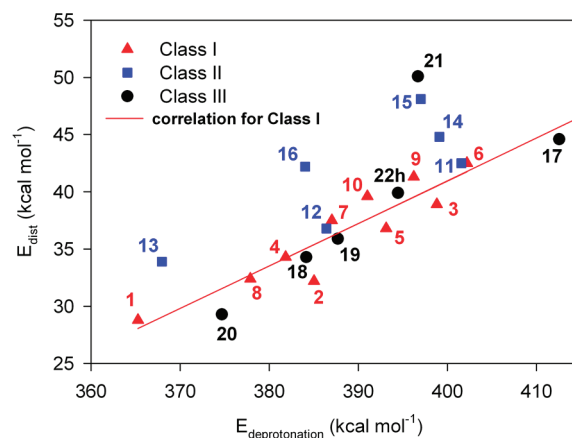


**Figure 6.** Arene distortion energies for the lowest-energy CMD TS structures with the  $[\text{Pd}(\text{C}_6\text{H}_5)(\text{PMe}_3)(\text{OAc})]$  catalyst as a function of the C–H bond deprotonation energies for substrates 1–22h (Class I arenes are red triangles, Class II arenes are blue squares, and Class III arenes are black circles). Linear correlation (red line) for Class I arenes is shown.

one (indolizine **21**) and for three Class II arenes out of six (indolizine **15**, imidazopyrimidine **16** and thiazole-*N*-oxide **13** show significantly higher distortion energies than those expected from eq 5).

**Metal–Arene Interaction Energy.** The evaluation of the electronic interaction ( $E_{\text{int}}$ ) when the metal catalyst and the arene in their CMD transition state geometry are brought together remains elusive. Generally speaking, the interaction energy for the CMD process results from two interactions: the metal–C(arene) interaction and the interaction of the base ligand with the partially cleaved C–H bond. For C2-substituted thiophenes, we have shown that the  $E_{\text{int}}$  is linked to nucleophilicity (Figure 4). The principal difficulty resides in the fact that there is little data available to assess the nucleophilicity of different carbon sites in (hetero)arene structures. The solution may be found in the development of a quantitative method that easily allows the evaluation of carbon site nucleophilicities.

## CONCLUSION

Distortion–interaction analysis of the C–H bond cleavage of a wide range of (hetero)aromatics through the concerted metalation–deprotonation pathway has been performed in an attempt to quantify the contributions to the CMD reactivity. On the basis of this analysis, all (hetero)arene substrates can be divided into three classes. For Class I arenes, the regioselectivity of C–H bond functionalization is controlled by the difference in the arene distortion energies. Class II includes the (hetero)arenes for which interaction energies with the metal catalyst are the determining factor in reactivity. Class III arenes are the (hetero)arenes in which both the distortion and interaction energies influence the C–H bond functionalization. This classification of the (hetero)arenes allows for an easier understanding of their reactivity.

The analysis of the CMD reaction pathway reveals that for some electron-rich and simple heteroarenes  $\pi$ -complexes are formed prior to the C–H bond cleavage step. In such intermediates, the arene fragments undergo only small distortion, refuting the idea of the formation of a Wheland intermediate that would possess strong Pd–(hetero)arene interaction.



The analysis of the bond interactions in the TS structures using a More O'Ferrall–Jencks diagram allows for the assessment of how concerted metalation–deprotonation depends on the nature of the (hetero)arene and the metal catalyst.

The effects of remote C2 substituents on the reactivity of thiophenes were evaluated. The computed trends in the reactivity were corroborated by experimental competition studies using six thiophenes. Nucleophilicity of thiophenes evaluated by the Hammett  $\sigma_p$  values appears to correlate with not just the catalyst–substrate interaction energies but also with the distortion energies of the substrate and of the catalyst.

Initial stepping stones were placed in the development of predictive guidelines for the activation of C–H bond functionalization catalyzed by Pd<sup>II</sup>-acetate catalysts. It has been shown that there is a correlation between the deprotonation energy of the (hetero)arenes and the distortion energy of arene in the CMD process. The C–H bond out-of-plane bending energy penalty for different arenes was found to have a fairly constant value. The principal remaining challenge to the development of the guidelines is to quantify the relationship between the nucleophilicity of (hetero)arenes and the energy of the interaction of the catalyst and (hetero)arene. Nevertheless, we believe that the findings in this work will be of practical use for future reaction development. We have presented where our conception of the CMD pathway stands and hope that this work will inspire new ideas and discoveries in the field of C–H bond functionalization.

## EXPERIMENTAL SECTION

**Computational Details.** Density functional theory (DFT) calculations have been performed using the Gaussian 03 program.<sup>38</sup> In all calculations, the spin-restricted method was employed. Wave function stability calculations were performed to confirm that the calculated wave functions corresponded to the electronic ground state. The structures of all species were optimized using the B3LYP exchange–correlation (XC) functional<sup>39,40</sup> with the mixed double/triple- $\zeta$  basis set (DZVP<sup>41</sup> on Pd and Rh, LANL2DZ basis set and effective-core potential on Ir, and TZVP<sup>42</sup> on all other atoms). Tight SCF convergence criteria ( $10^{-8}$  au) were used for all calculations. Harmonic frequency calculations with the analytic evaluation of force gradients were used to determine the nature of the stationary points. Intrinsic reaction coordinate (IRC)<sup>43,44</sup> calculations were used to confirm the reaction pathways through the CMD transition states (TSs) for all reactants. Gibbs free energies of species were evaluated at 298 K and 1 atm.

Mayer bond orders,<sup>45</sup> orbital populations, and compositions were calculated using Mulliken population analysis (MPA)<sup>46</sup> and the AOMix program.<sup>47</sup>

**Preparation of the 2'-(PdPCy<sub>3</sub>Cl)-2-Aminobiphenyl (23) Precatalyst.** The preparation of the precatalyst was made following the procedures reported by Buchwald et al.<sup>34</sup> A mixture of Pd(OAc)<sub>2</sub> (420 mg, 1.87 mmol, 1.0 equiv) and freshly purified 2-amino-biphenyl (331 mg, 1.96 mmol, 1.05 equiv) in anhydrous toluene (12 mL, 0.15 M) was heated at 60 °C for 30 min under an argon atmosphere, at which point the initial red color of the solution faded and a gray precipitate had formed. After the reaction cooled to room temperature, toluene was removed with a pipet. The remaining solid was washed twice with toluene (~3 mL) and then suspended in dry acetone (12 mL). After addition of lithium chloride (226 mg, 5.34 mmol, 3.0 equiv, stored in a desiccator), the resulting slurry was stirred at room temperature under argon for 1 h to give a homogeneous solution. PCy<sub>3</sub> (500 mg, 1.78 mmol, 1.0 equiv) was then added slowly over 5 min. The PCy<sub>3</sub> was stored and weighed in the glovebox, although PCy<sub>3</sub> can be stored on benchtop if kept under inert atmosphere. The mixture was stirred at room temperature for 3–4 h, at which point a

significant amount of a gray precipitate in suspension had formed. The precipitate in suspension was then separated from solid LiCl by decantation, and the remaining LiCl was washed with dry acetone once. The acetone suspension was then stored for some time to let the precipitate settle. Most of the solvent was removed with a pipet and washed twice with ether (~5 mL). When most of the solvent was removed with a pipet, the remaining solvent was removed with a rotary vacuum evaporator and dried under vacuum. Yield: 850 mg, 1.44 mmol (80%). <sup>31</sup>P NMR (121 MHz CDCl<sub>3</sub>): 36.0, 33.8. (rotamers).

**General Procedure for the Direct Arylation of Heterocycles.**<sup>26b</sup> 2'-(PdPCy<sub>3</sub>Cl)-2-Aminobiphenyl (5 mol %), K<sub>2</sub>CO<sub>3</sub> (1.5 equiv), and PivOH (30 mol %) were weighed in air and placed in a screw-cap vial equipped with a magnetic stir bar. The heteroarene (1.1 equiv) and the aryl bromide (1.0 equiv), if a solid, were then added. The vial was purged with argon, and a solution of the coupling partners, if liquid, in dimethylacetamide (DMA) (0.3 M) was added to the mixture. The reaction mixture was then stirred vigorously at 100 °C for 4–16 h. The solution was then cooled to ambient temperature and loaded directly on the column or was diluted with ethyl acetate, then filtered, and evaporated under reduced pressure. The crude product was purified by silica gel column chromatography to afford the corresponding product.

**General Procedure of the Competition Experiments of Figure 3, with the Exception of the Competitions Involving 1-(Thiophene-2-yl)pyrrolidine (22a).** 2'-(PdPCy<sub>3</sub>Cl)-2-Aminobiphenyl (23) (3.5 mg, 0.006 mmol, 1 mol %), K<sub>2</sub>CO<sub>3</sub> (83 mg, 0.60 mmol, 1.0 equiv), and PivOH (9.2 mg, 0.09 mmol, 15 mol %) were weighed in air and placed in a screw-cap vial equipped with a magnetic stir bar. The heteroarenes (0.30 mmol, 0.50 equiv each), if a solid, were then added. The vial was purged with argon, and a solution of the 5-bromo-*m*-xylene (11.1 mg, 0.060 mmol, 10 mol %) and the heteroarene (0.30 mmol, 0.5 equiv each), if liquid, in dimethylacetamide (2.0 mL, 0.3 M) was added to the mixture. The reaction mixture was then stirred vigorously at 100 °C overnight. The solution was then cooled to ambient temperature and then filtered and evaporated under reduced pressure. The remaining solvent was then removed under reduced pressure using a Kugelrohr apparatus. The crude mixture was then analyzed by <sup>1</sup>H NMR spectroscopy.

**General Procedure of the Competition Experiments of Figure 3 Involving 1-(Thiophene-2-yl)pyrrolidine (22a).** Due to the instability of 22a, an electron-deficient aryl bromide needed to be employed to give greater stability to the arylation product. 2'-(PdPCy<sub>3</sub>Cl)-2-Aminobiphenyl (23) (3.5 mg, 0.006 mmol, 1 mol %), K<sub>2</sub>CO<sub>3</sub> (83 mg, 0.60 mmol, 1.0 equiv), and PivOH (9.2 mg, 0.09 mmol, 15 mol %) were weighed in air and placed in a screw-cap vial equipped with a magnetic stir bar. The heteroarenes (0.30 mmol, 0.50 equiv each), if a solid, were then added. The vial was purged with argon and a solution of the 1-bromo-4-(trifluoromethyl)benzene (13.5 mg, 0.060 mmol, 10 mol %) and the heteroarenes (0.30 mmol, 0.5 equiv each), if liquid, in dimethylacetamide (2.0 mL, 0.3 M) was added to the mixture. The reaction mixture was then stirred vigorously at 100 °C overnight. The solution was then cooled to ambient temperature and then filtered and evaporated under reduced pressure. The remaining solvent was then removed under reduced pressure using a Kugelrohr apparatus. The crude mixture was then analyzed by <sup>1</sup>H NMR spectroscopy.

**1-(Thiophene-2-yl)pyrrolidine (22a).** Synthesized following a known procedure from 2-iodothiophene on a 10 mmol scale.<sup>48</sup> Variable yield depending on the batch: ~40–50%, 600–770 mg, ~4–5 mmol. Light-sensitive oil; *R*<sub>f</sub> 0.35 (petroleum ether/ethyl acetate 80/20); <sup>1</sup>H NMR (400 MHz, CDCl<sub>3</sub>)  $\delta$  ppm 6.78 (ddd, *J* = 5.2, 3.8, 1.2 Hz, 1H), 6.38 (dd, *J* = 5.4, 1.2 Hz, 1H), 5.75 (dd, *J* = 3.7, 1.2 Hz, 1H), 3.25 (dq, *J* = 6.5, 3.4 Hz, 4H), 2.05–1.97 (m, 4H); <sup>13</sup>C NMR (100 MHz, CDCl<sub>3</sub>)  $\delta$  ppm 155.9, 126.9, 108.3, 100.0, 51.2, 25.8; IR ( $\nu_{\max}$ /cm<sup>-1</sup>) 2966, 2889, 2837, 1533, 1471, 1456, 1362 cm<sup>-1</sup>; HRMS calcd for C<sub>8</sub>H<sub>11</sub>NS (M<sup>+</sup>) 153.0612, found 153.0614.

**5-(3,5-Dimethylphenyl)thiophene-2-carbonitrile.** Synthesized according to the general procedure for the direct arylation on a 0.50 mmol scale. Yield: 65 mg, 0.31 mmol (62%). Yellow solid, mp 68–70 °C (CHCl<sub>3</sub>); *R*<sub>f</sub> 0.60 (petroleum ether/ethyl acetate 80/20); <sup>1</sup>H NMR



(400 MHz, CDCl<sub>3</sub>)  $\delta$  ppm 7.57 (d,  $J$  = 3.9 Hz, 1H), 7.24 (d,  $J$  = 3.9 Hz, 1H), 7.21 (s, 2H), 7.04 (s, 1H), 2.36 (s, 6H); <sup>13</sup>C NMR (100 MHz, CDCl<sub>3</sub>)  $\delta$  ppm 152.4, 139.1, 138.4, 132.3, 131.3, 129.8, 124.4, 123.2, 114.7, 21.4; IR ( $\nu_{\max}$  /cm<sup>-1</sup>) 3084, 2961, 2358, 2331, 2219, 1652 cm<sup>-1</sup>; HRMS calcd for C<sub>13</sub>H<sub>11</sub>NS (M<sup>+</sup>) 213.0612, found 213.0618.

**Isopropyl 5-(3,5-Dimethylphenyl)thiophene-2-carboxylate.** Synthesized according to the general procedure for the direct arylation on a 0.50 mmol scale. Yield: 132 mg, 0.48 mmol (96%). Pale oil;  $R_f$  0.50 (petroleum ether/ethyl acetate 80/20); <sup>1</sup>H NMR (400 MHz, CDCl<sub>3</sub>)  $\delta$  ppm 7.73 (d,  $J$  = 3.9 Hz, 1H), 7.25 (s, 2H), 7.25 (d,  $J$  = 4.1 Hz, 1H), 6.99 (s, 1H), 5.22 (septuplet,  $J$  = 6.3 Hz, 1H), 2.35 (s, 6H), 1.36 (d,  $J$  = 6.3 Hz, 6H); <sup>13</sup>C NMR (100 MHz, CDCl<sub>3</sub>)  $\delta$  ppm 162.0, 151.5, 138.8, 134.1, 133.5, 132.8, 130.6, 124.2, 123.4, 68.8, 22.1, 21.4; IR ( $\nu_{\max}$  /cm<sup>-1</sup>) 2979, 2926, 2875, 1697, 1276 cm<sup>-1</sup>; HRMS calcd for C<sub>16</sub>H<sub>18</sub>O<sub>2</sub>S (M<sup>+</sup>) 274.1028, found 274.1050.

**2-Chloro-5-(3,5-dimethylphenyl)thiophene.** Synthesized according to the general procedure for the direct arylation. Yield: 109 mg, 0.489 mmol (98%). Green solid, mp 70–71 °C (CHCl<sub>3</sub>);  $R_f$  0.65 (petroleum ether/ethyl acetate 80/20); <sup>1</sup>H NMR (400 MHz, CDCl<sub>3</sub>)  $\delta$  ppm 7.12 (wide s, 2H), 7.02 (d,  $J$  = 3.9 Hz, 1H), 6.93 (wide s, 1H), 6.86 (d,  $J$  = 3.9 Hz, 1H), 2.33 (s, 6H); <sup>13</sup>C NMR (100 MHz, CDCl<sub>3</sub>)  $\delta$  ppm 143.4, 138.7, 133.7, 129.7, 128.8, 127.1, 123.6, 122.1, 21.4; IR ( $\nu_{\max}$  /cm<sup>-1</sup>) 2914, 2850, 1598, 1431 cm<sup>-1</sup>; HRMS calcd for C<sub>12</sub>H<sub>11</sub>ClS (M<sup>+</sup>) 222.0270, found 222.0254.

**1-(5-(3,5-Dimethylphenyl)thiophen-2-yl)ethanone.** Synthesized according to the general procedure for the direct arylation on a 0.30 mmol scale. Yield: 28 mg, 0.12 mmol (40%). Clear oil;  $R_f$  0.30 (petroleum ether/ethyl acetate 80/20); <sup>1</sup>H NMR (400 MHz, CDCl<sub>3</sub>)  $\delta$  ppm 7.64 (d,  $J$  = 4.0 Hz, 1H), 7.28 (d,  $J$  = 4.0 Hz, 1H), 7.27 (wide s, 2H), 7.00 (wide s, 1H), 2.55 (s, 3H), 2.35 (d,  $J$  = 0.6 Hz, 6H); <sup>13</sup>C NMR (100 MHz, CDCl<sub>3</sub>)  $\delta$  ppm 153.4, 142.8, 138.8, 133.5, 133.3, 130.9, 127.3, 124.3, 123.8, 26.7, 21.4; IR ( $\nu_{\max}$  /cm<sup>-1</sup>) 3004, 2921, 2864, 1647, 1436 cm<sup>-1</sup>; HRMS calcd for C<sub>14</sub>H<sub>14</sub>OS (M<sup>+</sup>) 230.0765, found 230.0761.

**2-(3,5-Dimethylphenyl)-5-propylthiophene.** Synthesized according to the general procedure for the direct arylation on a 0.30 mmol scale. Yield: 50.5 mg, 0.22 mmol (73%). Oil;  $R_f$  0.70 (petroleum ether/ethyl acetate 80/20); <sup>1</sup>H NMR (400 MHz, CDCl<sub>3</sub>)  $\delta$  ppm 7.18 (s, 2H), 7.09 (d,  $J$  = 3.5 Hz, 1H), 6.88 (s, 1H), 6.72 (dd,  $J$  = 3.5, 1.9 Hz, 1H), 2.79 (t,  $J$  = 7.5 Hz, 2H), 2.33 (s, 6H), 1.72 (sextet,  $J$  = 7.4 Hz, 2H), 1.00 (t,  $J$  = 7.3 Hz, 3H); <sup>13</sup>C NMR (100 MHz, CDCl<sub>3</sub>)  $\delta$  ppm 145.2, 142.1, 138.4, 134.7, 128.9, 125.1, 123.6, 122.6, 32.5, 25.0, 21.5, 13.8; IR ( $\nu_{\max}$  /cm<sup>-1</sup>) 2962, 2922, 2870, 1652, 1558 cm<sup>-1</sup>; HRMS calcd for C<sub>15</sub>H<sub>18</sub>S (M<sup>+</sup>) 230.1129, found 230.1121.

**1-(5-(4-(Trifluoromethyl)phenyl)thiophen-2-yl)pyrrolidine.** Synthesized according to the general procedure for the direct arylation on a 0.30 mmol scale. Yield: 56.4 mg, 0.19 mmol (63%). Green solid, mp 142–144 °C (CHCl<sub>3</sub>);  $R_f$  0.25 (petroleum ether/ethyl acetate 80/20); <sup>1</sup>H NMR (300 MHz, CDCl<sub>3</sub>)  $\delta$  ppm 7.53–7.47 (m, 4H), 7.16 (d,  $J$  = 3.9 Hz, 1H), 5.73 (d,  $J$  = 4.0 Hz, 1H), 3.34–3.30 (m, 4H), 2.08–2.03 (m, 4H); <sup>13</sup>C NMR (100 MHz, CDCl<sub>3</sub>)  $\delta$  ppm 156.2, 139.1, 126.5 (q,  $J_{C-F}$  = 32.0 Hz), 125.8 (q,  $J_{C-F}$  = 3.9 Hz), 125.1, 124.6 (q,  $J_{C-F}$  = 272.1 Hz), 124.1, 123.6, 101.6, 51.0, 25.9; IR ( $\nu_{\max}$  /cm<sup>-1</sup>) 3055, 2985, 2856, 1610, 1517, 1481, 1326, 1107 cm<sup>-1</sup>; HRMS calcd for C<sub>15</sub>H<sub>14</sub>F<sub>3</sub>NS (M<sup>+</sup>) 297.0799, found 297.0792.

**5-(4-(Trifluoromethyl)phenyl)thiophene-2-carbonitrile.** Synthesized according to the general procedure for the direct arylation on a 0.50 mmol scale. Yield: 92 mg, 0.363 mmol (73%). <sup>1</sup>H NMR of the final product matched the previously reported spectrum.<sup>49</sup> Yellow solid;  $R_f$  0.10 (petroleum ether/diethyl ether 95/5); <sup>1</sup>H NMR (400 MHz, CDCl<sub>3</sub>)  $\delta$  ppm 7.73–7.68 (m, 4H), 7.63 (d,  $J$  = 3.9 Hz, 1H), 7.36 (d,  $J$  = 3.9 Hz, 1H).

**Isopropyl 5-(4-(Trifluoromethyl)phenyl)thiophene-2-carboxylate.** Synthesized according to the general procedure for the direct arylation on a 0.50 mmol scale. Yield: 105 mg, 0.336 mmol (67%). White solid, mp 96–98 °C (CHCl<sub>3</sub>);  $R_f$  0.60 (petroleum ether/ethyl acetate 80/20); <sup>1</sup>H NMR (400 MHz, CDCl<sub>3</sub>)  $\delta$  ppm 7.77 (d,  $J$  = 3.9 Hz, 1H), 7.74 (d,  $J$  = 8.1 Hz, 2H), 7.66 (d,  $J$  = 8.3 Hz, 2H), 7.36 (d,  $J$  = 3.9 Hz, 1H), 5.24 (7,  $J$  = 6.3 Hz, 1H), 1.38 (d,  $J$  = 6.3 Hz,

6H); <sup>13</sup>C NMR (100 MHz, CDCl<sub>3</sub>)  $\delta$  ppm 161.7, 148.8, 137.0, 134.7, 134.1, 130.5 (q,  $J_{C-F}$  = 33.0 Hz), 126.5 (q,  $J_{C-F}$  = 3.8 Hz), 126.2, 124.9, 124.2 (q,  $J_{C-F}$  = 272.1 Hz), 69.2, 22.1; IR ( $\nu_{\max}$  /cm<sup>-1</sup>) 3002, 2993, 1679, 1653, 1276 cm<sup>-1</sup>; HRMS calcd for C<sub>15</sub>H<sub>13</sub>F<sub>3</sub>O<sub>2</sub>S (M<sup>+</sup>) 314.0588, found 314.0589.

**2-Chloro-5-(4-(trifluoromethyl)phenyl)thiophene.** Synthesized according to the general procedure for the direct arylation. <sup>1</sup>H NMR of the final product matched the previously reported spectrum.<sup>4</sup> Pale yellow solid;  $R_f$  0.60 (petroleum ether/ethyl acetate 95/5); <sup>1</sup>H NMR (400 MHz, CDCl<sub>3</sub>)  $\delta$  ppm 7.64–7.59 (m, 4H), 7.16 (d,  $J$  = 3.9 Hz, 1H), 6.93 (d,  $J$  = 3.9 Hz, 1H).

**1-(5-(4-(Trifluoromethyl)phenyl)thiophen-2-yl)ethanone.** Synthesized according to the general procedure for the direct arylation on a 0.50 mmol scale. Yield: 68 mg, 0.25 mmol (50%). <sup>1</sup>H NMR of the final product matched the previously reported spectrum.<sup>49</sup> White solid;  $R_f$  0.35 (petroleum ether/ethyl acetate 70/30); <sup>1</sup>H NMR (400 MHz, CDCl<sub>3</sub>)  $\delta$  ppm 7.76 (d,  $J$  = 8.2 Hz, 2H), 7.68 (d,  $J$  = 3.9 Hz, 2H), 7.67 (d,  $J$  = 8.3 Hz, 1H), 7.40 (d,  $J$  = 4.0 Hz, 1H), 2.59 (s, 3H).

**2-Propyl-5-(4-(trifluoromethyl)phenyl)thiophene.** Synthesized according to the general procedure for the direct arylation. <sup>1</sup>H NMR of the final product matched the previously reported spectrum.<sup>26b</sup> <sup>1</sup>H NMR (400 MHz, CDCl<sub>3</sub>)  $\delta$  ppm 7.64 (d,  $J$  = 8.4 Hz, 2H), 7.59 (d,  $J$  = 8.4 Hz, 2H), 7.21 (d,  $J$  = 3.6 Hz, 1H), 6.78 (d,  $J$  = 3.5 Hz, 1H), 2.81 (t,  $J$  = 7.5 Hz, 2H), 1.74 (sext,  $J$  = 7.5 Hz, 2H), 1.01 (t,  $J$  = 7.3 Hz, 3H).

## ■ ASSOCIATED CONTENT

### 📄 Supporting Information

Cartesian coordinates and absolute energies of CMD transition states, the results of distortion–interaction analysis, and spectroscopic characterization of the reactants and products. This material is available free of charge via the Internet at <http://pubs.acs.org>.

## ■ AUTHOR INFORMATION

### ✉ Corresponding Author

\*E-mail: [sgorelsk@uottawa.ca](mailto:sgorelsk@uottawa.ca); [dlapo063@uottawa.ca](mailto:dlapo063@uottawa.ca).

### Notes

<sup>†</sup>Prof. Keith Fagnou passed away on November 11, 2009.

## ■ ACKNOWLEDGMENTS

The authors thank Thomas Markiewicz for his help in the preparation of this manuscript. We thank NSERC, CCRI, and the University of Ottawa for supporting this work. D.L. thanks NSERC for a postgraduate scholarship (PGS-D).

## ■ REFERENCES

- (1) (a) Daugulis, O.; Zaitsev, V. G.; Shabashov, D.; Pham, Q.-N.; Lazareva, A. *Synlett* **2006**, 3382. (b) Campeau, L.-C.; Fagnou, K. *Chem. Commun.* **2006**, 1253. (c) Alberico, D.; Scott, M. E.; Lautens, M. *Chem. Rev.* **2007**, *107*, 174. (d) Seregin, I. V.; Gevorgyan, V. *Chem. Soc. Rev.* **2007**, *36*, 1173. (e) Satoh, T.; Miura, M. *Chem. Lett.* **2007**, *36*, 200. (f) Campeau, L.-C.; Stuart, D. R.; Fagnou, K. *Aldrichimica Acta* **2007**, *40*, 35. (g) Li, B.-J.; Yang, S.-D.; Shi, Z.-J. *Synlett* **2008**, 949. (h) Kakiuchi, F.; Kochi, T. *Synthesis* **2008**, 3013. (i) McGlacken, G. P.; Bateman, L. M. *Chem. Soc. Rev.* **2009**, *38*, 2447. (j) Chen, X.; Engle, K. M.; Wang, D.-H.; Yu, J.-Q. *Angew. Chem., Int. Ed.* **2009**, *48*, 5094. (k) Kulkarni, A. A.; Daugulis, O. *Synthesis* **2009**, *24*, 4087. (l) Bellina, F.; Rossi, R. *Tetrahedron* **2009**, *65*, 10269. (m) Ackermann, L.; Vicente, R.; Kapdi, A. R. *Angew. Chem., Int. Ed.* **2009**, *48*, 9792. (n) Roger, J.; Gottumukkala, A. L.; Doucet, H. *ChemCatChem* **2010**, *2*, 20. (o) Lyons, T. W.; Sanford, M. S. *Chem. Rev.* **2010**, *110*, 1147.
- (2) García-Cuadrado, D.; de Mendoza, P.; Braga, A. A. C.; Maseras, F.; Echavarren, A. M. *J. Am. Chem. Soc.* **2007**, *129*, 6880.

(3) (a) Lafrance, M.; Rowley, C. N.; Woo, T. K.; Fagnou, K. *J. Am. Chem. Soc.* **2006**, *128*, 8754. (b) Guihaume, J.; Clot, E.; Eisenstein, O.; Perutz, R. N. *Dalton Trans.* **2010**, *39*, 10510.

(4) Liégault, B.; Petrov, I.; Gorelsky, S. I.; Fagnou, K. *J. Org. Chem.* **2010**, *75*, 1047.

(5) Caron, L.; Campeau, L.-C.; Fagnou, K. *Org. Lett.* **2008**, *10*, 4533.

(6) Campeau, L.-C.; Stuart, D. R.; Leclerc, J.-P.; Bertrand-Laperle, M.; Villemure, É.; Sun, H.-Y.; Lasserre, S.; Guimond, N.; Lecavallier, M.; Fagnou, K. *J. Am. Chem. Soc.* **2009**, *131*, 3291.

(7) Campeau, L.-C.; Parisien, M.; Jean, A.; Fagnou, K. *J. Am. Chem. Soc.* **2006**, *128*, 581.

(8) Lane, B. S.; Brown, M. A.; Sames, D. *J. Am. Chem. Soc.* **2005**, *127*, 8050.

(9) Sun, H.-Y.; Gorelsky, S. I.; Stuart, D. R.; Campeau, L.-C.; Fagnou, K. *J. Org. Chem.* **2010**, *75*, 8180.

(10) For consistency with our previous reports, we have chosen to employ the CMD acronym to describe the metal-carboxylate catalyzed C–H bond cleavage mechanism. Some authors use other terms, such as internal electrophilic substitution (IES) and ambiphilic metal–ligand activation (AMLA) to describe this mechanism; see: (a) Oxgaard, J.; Tenn, W. J. III; Nielsen, R. J.; Periana, R. A.; Goddard, W. A. III *Organometallics* **2007**, *26*, 1565. (b) Boutadla, Y.; Davies, D. L.; Macgregor, S. A.; Poblador-Bahamonde, A. I. *Dalton Trans.* **2009**, 5887.

(11) For recent reviews on metal-carboxylate promoted concerted metalation/C–H bond cleavage, see: (a) Boutadla, Y.; Davies, D. L.; Macgregor, S. A.; Poblador-Bahamonde, A. I. *Dalton Trans.* **2009**, 5820. (b) Lapointe, D.; Fagnou, K. *Chem. Lett.* **2010**, *39*, 1118. (c) Ackermann, L. *Chem. Rev.* **2011**, *111*, 1315.

(12) Kirchberg, S.; Tani, S.; Ueda, K.; Yamaguchi, J.; Studer, A.; Itami, K. *Angew. Chem., Int. Ed.* **2011**, *50*, 2387.

(13) Fung, C. W.; Khorramdel-Vahed, M.; Ranson, R. J.; Roberts, R. M. G. *J. Chem. Soc., Perkin Trans. 2* **1980**, 267.

(14) Biswas, B.; Sugimoto, M.; Sakaki, S. *Organometallics* **2000**, *19*, 3895.

(15) Lafrance, M.; Fagnou, K. *J. Am. Chem. Soc.* **2006**, *128*, 16496.

(16) Tan, Y.; Hartwig, J. F. *J. Am. Chem. Soc.* **2011**, *133*, 3308.

(17) González, J. J.; García, N.; Gómez-Lor, B.; Echavarren, A. M. *J. Org. Chem.* **1997**, *62*, 1286.

(18) Gorelsky, S. I.; Lapointe, D.; Fagnou, K. *J. Am. Chem. Soc.* **2008**, *130*, 10848.

(19) (a) Stuart, D. R.; Fagnou, K. *Science* **2007**, *316*, 1172. (b) Stuart, D. R.; Villemure, E.; Fagnou, K. *J. Am. Chem. Soc.* **2007**, *129*, 12072.

(c) Potavathri, S.; Pereira, K. C.; Gorelsky, S. I.; Pike, A.; LeBris, A. P.; DeBoef, B. *J. Am. Chem. Soc.* **2010**, *132*, 14676.

(20) Meir, R.; Kozuch, S.; Uhe, A.; Shaik, S. *Chem.—Eur. J.* **2011**, *17*, 7623.

(21) Lapointe, D.; Markiewicz, T.; Whipp, C. J.; Toderian, A.; Fagnou, K. *J. Org. Chem.* **2011**, *76*, 749.

(22) (a) Gorelsky, S. I.; Ghosh, S.; Solomon, E. I. *J. Am. Chem. Soc.* **2006**, *128*, 278. (b) Ess, D. N.; Houk, K. N. *J. Am. Chem. Soc.* **2007**, *129*, 10646. (c) van Zeist, W.-J.; Bickelhaupt, F. M. *Org. Biomol. Chem.* **2010**, *8*, 3118.

(23) (a) Becke, A. D. *J. Chem. Phys.* **1993**, *98*, 5648. (b) Lee, C.; Yang, W.; Parr, R. G. *Phys. Rev.* **1988**, *B37*, 785.

(24) Do, H.-Q.; Kashif Khan, R. M.; Daugulis, O. *J. Am. Chem. Soc.* **2008**, *130*, 15185.

(25) Several reports on the C–H functionalization reported various *o:m:p* ratios of product under various conditions; see ref 15 and (a) Brasche, G.; García-Fortanet, J.; Buchwald, S. L. *Org. Lett.* **2008**, *10*, 2207. (b) Yeung, C. S.; Zhao, X.; Borduas, N.; Dong, V. M. *Chem. Sci* **2010**, *1*, 331. (c) Wang, X.; Leow, D.; Yu, J.-Q. *J. Am. Chem. Soc.* **2011**, *133*, 13864.

(26) For substrates 1–3, see ref 3; for 5, see (a) Campeau, L.-C.; Rousseaux, S.; Fagnou, K. *J. Am. Chem. Soc.* **2005**, *127*, 18020. For 7, 10–12, 14–16, 21, and 22, see: (b) Liégault, B.; Lapointe, D.; Caron, L.; Vlassova, A.; Fagnou, K. *J. Org. Chem.* **2009**, *74*, 1826 and references therein. For 9, see: (c) Goikhman, R.; Jacques, T. L.; Sames, D. *J. Am. Chem. Soc.* **2009**, *131*, 3042. For 13, 19 and 20, see ref 6. For 17, see

ref 15. For 18, see: (d) Leclerc, J.-P.; Fagnou, K. *Angew. Chem., Int. Ed.* **2006**, *45*, 7781.

(27) For a report of the copper-catalyzed C2 arylation of 4, see: Do, H.-Q.; Khan, R. M. K.; Daugulis, O. *J. Am. Chem. Soc.* **2008**, *130*, 15185.

(28) (a) Ess, D. H.; Bischof, S. M.; Oxgaard, J.; Periana, R. A.; Goddard, W. A. III *Organometallics* **2008**, *27*, 6440. (b) Bischof, S. M.; Ess, D. H.; Meier, S. K.; Oxgaard, J.; Nielsen, R. J.; Bhalla, G.; Goddard, W. A. III; Periana, R. A. *Organometallics* **2010**, *29*, 742.

(29) Joo, J. M.; Tourré, B. B.; Sames, D. *J. Org. Chem.* **2010**, *75*, 4911.

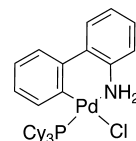
(30) (a) More O'Ferrall, R. A. *J. Chem. Soc. B* **1970**, 274. (b) Jencks, W. P. *Chem. Rev.* **1972**, *72*, 705.

(31) The reaction with the  $[\text{Ir}(\text{C}_5\text{H}_5)(\text{PMe}_3)(\text{CO}_3)]$  complex was evaluated on the basis of published results for a similar  $\text{Ir}^{\text{III}}$  complex with dimethylbenzylamine; see: Davies, D. L.; Donald, S. M. A.; Al-Duajj, O.; Macgregor, S. A.; Pölleth, M. *J. Am. Chem. Soc.* **2006**, *128*, 4210. For discussion of arylation of benzene, thiophenes, furans, and indoles using the  $[\text{Ir}(\text{PMe}_3)(\text{py})(\text{C}_6\text{H}_5)(\text{CO}_3)]$  catalyst, see: Garcia-Melchor, M.; Gorelsky, S. I.; Woo, T. K. *Chem.—Eur. J.* **2011**, *17*, 13847.

(32) Guimond, N.; Gorelsky, S. I.; Fagnou, K. *J. Am. Chem. Soc.* **2011**, *133*, 6449.

(33) Ferrer Flegeau, E.; Bruneau, C.; Dixneuf, P. H.; Jutand, A. *J. Am. Chem. Soc.* **2011**, *133*, 10161.

(34) Compound 23 was prepared following a procedure reported by Buchwald; Kinzel, T.; Zhang, Y.; Buchwald, S. L.; et al. *J. Am. Chem. Soc.* **2010**, *132*, 14073.



(35) A reaction of direct arylation performed with 1.0 equiv of 5-bromo-*m*-xylene and 1.1 equiv of thiophene yielded full conversion of aryl bromide and 1:2.8 mixtures of mono and double arylation products, respectively. The same reaction with 5.0 equiv of thiophene yielded a 1.2:1 mixture of the same products.

(36) Hansch, C.; Leo, A.; Taft, R. W. *Chem. Rev.* **1991**, *91*, 165.

(37) (a) Ryabov, A. D.; Sakodinskaya, I. K.; Yatsimirsky, A. K. *J. Chem. Soc., Dalton Trans.* **1985**, 2629. (b) Shilov, A. E.; Shul'pin, G. B. *Chem. Rev.* **1997**, *97*, 2879.

(38) Frisch, M. J.; Trucks, G. W.; Schlegel, H. B.; Scuseria, G. E.; Robb, M. A.; Cheeseman, J. R.; Montgomery, J. A.; Vreven, T.; Kudin, K. N.; Burant, J. C.; Millam, J. M.; Lyengar, S. S.; Tomasi, J.; Barone, V.; Mennucci, B.; Cossi, M.; Scalmani, G.; Rega, N.; Petersson, G. A.; Nakatsuji, H.; Hada, M.; Ehara, M.; Toyota, K.; Fukuda, R.; Hasegawa, J.; Ishida, M.; Nakajima, T.; Honda, Y.; Kitao, O.; Nakai, H.; Klene, M.; Li, X.; Knox, J. E.; Hratchian, H. P.; Cross, J. B.; Adamo, C.; Jaramillo, J.; Gomperts, R.; Stratmann, R. E.; Yazyev, O.; Austin, A. J.; Cammi, R.; Pomelli, C.; Ochterski, J. W.; Ayala, P. Y.; Morokuma, K.; Voth, G. A.; Salvador, P.; Dannenberg, J. J.; Zakrzewski, V. G.; Dapprich, S.; Daniels, A. D.; Strain, M. C.; Farkas, O.; Malick, D. K.; Rabuck, A. D.; Raghavachari, K.; Foresman, J. B.; Ortiz, J. V.; Cui, Q.; Baboul, A. G.; Clifford, S.; Cioslowski, J.; Stefanov, B. B.; Liu, G.; Liashenko, A.; Piskorz, P.; Komaromi, I.; Martin, R. L.; Fox, D. J.; Keith, T.; Al-Laham, M. A.; Peng, C. Y.; Nanayakkara, A.; Challacombe, M.; Gill, P. M. W.; Johnson, B.; Chen, W.; Wong, M. W.; Gonzalez, C.; Pople, J. A. *Gaussian 03, Revision C.01*; Gaussian, Inc.: Wallingford, CT, 2003.

(39) Becke, A. D. *J. Chem. Phys.* **1993**, *98*, 5648.

(40) Lee, C.; Yang, W.; Parr, R. G. *Phys. Rev.* **1988**, *B37*, 785.

(41) Godbout, N.; Salahub, D. R.; Andzelm, J.; Wimmer, E. *Can. J. Chem.* **1992**, *70*, 560.

(42) Schafer, A.; Huber, C.; Ahlrichs, R. *J. Chem. Phys.* **1994**, *100*, 5829.

(43) Gonzalez, C.; Schlegel, H. B. *J. Chem. Phys.* **1989**, *90*, 2154.

(44) Gonzalez, C.; Schlegel, H. B. *J. Phys. Chem.* **1990**, *94*, 5523.

- (45) (a) Mayer, I. *Chem. Phys. Lett.* **1983**, *97*, 270. (b) Gorelsky, S. I.; Basumallick, L.; Vura-Weis, J.; Sarangi, R.; Hedman, B.; Hodgson, K. O.; Fujisawa, K.; Solomon, E. I. *Inorg. Chem.* **2005**, *44*, 4947.
- (46) Mulliken, R. S. *J. Chem. Phys.* **1955**, *23*, 1833.
- (47) Gorelsky, S. I. *AOMix: Program for Molecular Orbital Analysis*, version 6.5; University of Ottawa: Ottawa, Canada, 2011 (<http://www.sg-chem.net>).
- (48) Lu, Z.; Twieg, R. J. *Tetrahedron* **2005**, *61*, 903.
- (49) Battace, A.; Lemhadri, M.; Zair, T.; Doucet, H.; Santelli, M. *Adv. Synth. Catal.* **2007**, *349*, 2507.